Environmental Science & Technology

Article

Cite This: Environ. Sci. Technol. 2019, 53, 5168−5175

pubs.acs.org/est

In Situ Quantification of Biological N_2 Production Using Naturally Occurring $^{15}N^{15}N$

Laurence Y. Yeung,*[,†] Joshua A. Haslun,[‡] Nathaniel E. Ostrom,[‡] Tao Sun,[†] Edward D. Young,[§] Maartje A. H. J. van Kessel,[∥] Sebastian Lücker,[∥] and Mike S. M. Jetten[∥]

[†]Department of Earth, Environmental and Planetary Sciences, Rice University, Houston, Texas 77005, United States

[‡]Department of Integrative Biology and Great Lakes Bioenergy Research Center, Michigan State University, East Lansing, Michigan 48824, United States

[§]Department of Earth, Planetary, and Space Sciences, University of California-Los Angeles, Los Angeles, California 90095, United States

[∥]Department of Microbiology, Radboud University, Nijmegen 6525 AJ, The Netherlands

Supporting Information

ABSTRACT: We describe an approach for determining biological N_2 production in soils based on the proportions of naturally occurring $^{15}N^{15}N$ in N_2. Laboratory incubation experiments reveal that biological N_2 production, whether by denitrification or anaerobic ammonia oxidation, yields proportions of $^{15}N^{15}N$ in N_2 that are within 1‰ of that predicted for a random distribution of ^{15}N and ^{14}N atoms. This relatively invariant isotopic signature contrasts with that of the atmosphere, which has $^{15}N^{15}N$ proportions in excess of the random distribution by 19.1 ± 0.1‰. Depth profiles of gases in agricultural soils from the Kellogg Biological Station Long-Term Ecological Research site show biological N_2 accumulation that accounts for up to 1.6% of the soil N_2. One-dimensional reaction-diffusion modeling of these soil profiles suggests that subsurface N_2 pulses leading to surface emission rates as low as 0.3 mmol N_2 m^{-2} d^{-1} can be detected with current analytical precision, decoupled from N_2O production.

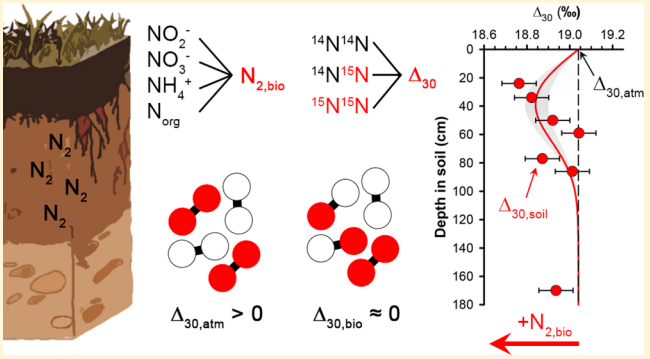

INTRODUCTION

Biological N_2 production constitutes the main mechanism through which fixed nitrogen is returned to the atmosphere. While many methods have been developed for measuring N_2 production in the field, obtaining accurate estimates of ecosystem fixed-nitrogen loss remains a challenge.[1,2] Field-based techniques often require nutrient amendments (e.g., ^{15}N-labeled nitrate), manipulation of biochemical pathways (e.g., C_2H_2 inhibition of nitrous oxide reductase),[3] or sampling and incubation of soil cores, all of which introduce poorly constrained uncertainties.[4,5] For example, in nutrient amendment studies, the fraction of extant nitrogen substrate utilized must be accounted for, but it is often difficult to constrain. Moreover, biological N_2 production can be stimulated by substrate addition, biasing measurements based on this approach. Soil-core incubations to evaluate N_2 production may not require nutrient amendments, but instead require that the extant gases be replaced with a gas mixture to reduce or replace the ambient N_2 background.[6] Ultimately, this suite of methods for quantifying N_2 production rates can only probe short-term and potential rates of denitrification and other nitrogen-loss processes. Importantly, they may not integrate variation in activity that occurs over longer time scales at a given sampling site. Passive in situ measurements are rare, and fraught with a different set of complications: a recent attempt to use N_2/Ar ratios to probe excess N_2 production in situ found that physical fractionation of gases, combined with insufficient sensitivity, would likely preclude its widespread application.[7]

Stable isotopes of nitrogen at natural abundance levels could in principle be used to determine the amount of biologically produced N_2 in soil gases as well. Variations in the $^{15}N/^{14}N$ ratio of N_2, reported as a δ-value in per mil (‰) relative to atmospheric N_2,

$$\delta^{15}N \equiv {}^{15}R_{sample}/{}^{15}R_{atm} - 1 \quad (1)$$

$$^{15}R = {}^{15}N/{}^{14}N \quad (2)$$

can be caused by variability in the chemistry of N_2 cycling, substrate $\delta^{15}N$, and physical transport. Nevertheless, a large isotopic contrast may exist between biological and atmospheric

Received: February 8, 2019
Revised: April 2, 2019
Accepted: April 4, 2019
Published: April 4, 2019

DOI: 10.1021/acs.est.9b00812
Environ. Sci. Technol. 2019, 53, 5168−5175

N_2: strong isotopic fractionation for N_2-yielding processes[8−10] can result in local deviations in the $\delta^{15}N$ value of N_2 relative to their substrates and the atmospheric background. However, closed-system and rate-dependent effects on isotopic fractionation,[11] the broad distribution of substrate $\delta^{15}N$ values,[12] and physical fractionation affecting the elemental and isotopic composition of soil gases[13] are rarely well-characterized, rendering the interpretation of bulk $\delta^{15}N$ values in soil N_2 nonunique; disentangling the variations in $\delta^{15}N$ of soil-N_2 may not be possible without additional constraints.

We recently developed methods to measure $^{15}N^{15}N$ in N_2 with high precision at natural abundances, which offers a new approach to quantifying in N_2 production on local and global scales.[14] Together with $^{14}N^{15}N/^{14}N^{14}N$ ratios, measurements of the $^{15}N^{15}N/^{14}N^{14}N$ ratio in N_2 yield a "clumped" isotope tracer, Δ_{30}, which is defined below and also reported in per mil:

$$\Delta_{30} \equiv {}^{30}R_{sample}/{}^{30}R_{random} - 1 \quad (3)$$

$${}^{30}R_{sample} = {}^{15}N^{15}N/{}^{14}N^{14}N \quad (4)$$

$${}^{30}R_{random} = ({}^{15}N/{}^{14}N)^2 \quad (5)$$

Unlike the $\delta^{15}N$ value, Δ_{30} represents the proportional (rather than absolute) enrichment in $^{15}N^{15}N$, quantified relative to a random distribution of ^{15}N and ^{14}N atoms in N_2 molecules. The $\delta^{15}N$ value of the substrate does not affect the Δ_{30} signature of a N_2-yielding process because the Δ_{30} value is normalized against the bulk $^{15}N/^{14}N$ ratio (eqs 3 and 5). Moreover, the Δ_{30} tracer is insensitive to physical fractionation and nitrogen fixation;[14,15] these processes tend to preserve proportions of $^{15}N^{15}N$ relative to $^{14}N^{15}N$ and $^{14}N^{14}N$. Furthermore, the Δ_{30} values of the biological N_2 thus far identified cluster near zero, while the Δ_{30} value of atmospheric N_2 is 19.1 ± 0.1‰—a signature of upper-atmospheric gas-phase reactions.[14] It results in a large isotopic contrast between biological and atmospheric N_2. Local subatmospheric Δ_{30} values in soils thus may reflect the presence of biological N_2, which can be quantified through a clumped-isotope mass balance if the Δ_{30} signatures of different N_2-producing pathways are sufficiently similar. Δ_{30} values may trace biological N_2 production in situ using the same principles first laid out by Hauck and co-workers,[16,17] but without the need for nutrient amendments or isotopic labels.

Motivated by this potential application, we conducted a broader survey of Δ_{30} values from biological processes. Specifically, we expanded our earlier characterization of Δ_{30} values from denitrifying bacteria[14] with new measurements of Δ_{30} signatures from anaerobic ammonia-oxidizing (anammox) bacteria and incubations of natural soils. The narrow distribution of biological Δ_{30} signatures that we find suggests that Δ_{30} values can indeed be used to quantify biological N_2 production in soils, and possibly also other restricted environments. As a proof-of-principle application, we present two soil-gas depth profiles that show evidence for biological N_2 production, and evaluate the sensitivity of the approach.

EXPERIMENTAL METHODS

Isotopic analyses were performed on the ultrahigh resolution Nu Instruments *Panorama* mass spectrometer at the University of California, Los Angeles according to methods described previously.[14,18] The uniquely high resolution of the instrument allows the simultaneous measurement of $^{14}N^{15}N^+/^{14}N^{14}N^+$ and $^{15}N^{15}N^+/^{14}N^{14}N^+$ ratios at m/z = 29 and 30, with near-baseline resolution of $^{15}N^{15}N^+$ from $^{14}N^{16}O^+$ and $^{12}C^{18}O$ at m/z = 30. N_2 gas samples (20−50 μmol) were isolated from experimental headspace and soil-derived gases using cryogenic purification on a high-vacuum sample preparation line followed by gas chromatographic separation from O_2 and Ar before isotopic analysis. Cryogenic purification removes condensable gases (e.g., CO_2 and some hydrocarbons) and was accomplished by passing the gas through a stainless-steel U-trap submerged in liquid nitrogen (−196 °C). The gas was then condensed onto silica gel pellets at −196 °C within the sample-injection loop of the gas-chromatographic system. N_2 gas was separated from O_2 and Ar using a molecular sieve 5A column (3 m × 1/8" OD) followed by a HayeSep D column (2 m × 1/8 in. OD) inline, all with a 20 mL min^{-1} He flow rate at 25 °C. The sample gases, air, and high-temperature standards of N_2 (which were heated at 800 °C for 24−48 h over strontium nitride) were purified the same way and analyzed during the same analytical sessions. Analytical precision for replicate air samples during these sessions was ±0.006‰ for $\delta^{15}N$ and ±0.08‰ for Δ_{30}.

To determine the Δ_{30} signatures of N_2 produced by anammox bacteria, headspace outflows from several anammox bioreactors at Radboud University were sampled. Outflows from bioreactors containing enrichment cultures of the genera *Candidatus Kuenenia*,[19] and *Ca. Brocadia*[20] (both freshwater genera), as well as *Ca. Scalindua*[21] (a marine genus) were sampled using a 8 mL sampling loop made of a 1/4 in. OD stainless steel tube. The gas mixture was transferred cryogenically to a pre-evacuated sample finger filled with silica gel at −196 °C for 15 min before flame-sealing. All enrichment cultures at Radboud University were grown on the same NH_4SO_4 + $NaNO_2$ substrates, which had $\delta^{15}N$ values of −0.5 ± 0.3‰ and −26.2 ± 0.3‰, respectively. Atmospheric contamination was monitored using gas chromatography−mass spectrometry of the outflow, using O_2 (m/z = 32) as a proxy. A correction for air-N_2 contamination in the bioreactor headspace was calculated from the O_2 signal and a proportionality coefficient determined through a series of volumetrically calibrated mixtures of air in the 95% Ar/5% CO_2 mixture used to flush the bioreactors. Measured air contamination varied between bioreactors, ranging from 0.6% for *Kuenenia* to 12.3% for *Scalindua* outflows, as a result of variable anammox activity compared to the flushing flow rate. After correction for background contamination (0.12−2.40‰ for $\delta^{15}N$ and 0.1−2.3‰ for Δ_{30}), duplicate collections showed reproducibility in $\delta^{15}N$ and Δ_{30} within ±0.01‰ and ±0.3‰, respectively.

Incubations of natural soils were performed to determine the Δ_{30} signatures of N_2 produced by natural biological communities. Soils from three agricultural treatments at the Kellogg Biological Station (KBS) Long-Term Ecological Research site were used for these experiments. Soils at the site belong to the Kalamazoo series, which are fine-loamy, mixed mesic Typic Hapludafs.[22] Soils T1 and T2 are agricultural soils that have been under an annual corn−soybean−winter wheat rotation since 1989, with T1 conventionally tilled with a chisel plow and T2 being no-till. Soil T7 comes from a native early successional old field community (containing grasses, shrubs, and trees) that was established in 1989 and has been maintained by an annual spring burn since 1997. Incubations of 25-g soil samples were conducted in 125 mL glass serum bottles that were crimp-sealed using butyl

DOI: 10.1021/acs.est.9b00812
Environ. Sci. Technol. 2019, 53, 5168−5175

Table 1. Clumped-Isotope Composition of N_2 ($\pm 1\sigma$) Derived from Experimental Cultures of Denitrifying or Anammox Bacteria

	substrate	Δ_{30} (‰)	n	Reference
natural soils				
KBS T1 (conventional agricultural)	KNO_3	−0.1 ± 0.1	3	this work
KBS T2 (no-till agricultural)	KNO_3	0.1 ± 0.3	3	this work
KBS T7 (early successional)	KNO_3	0.2 ± 0.2	4	this work
anammox enrichment cultures				
Kuenenia spp.	NH_4SO_4 + $NaNO_2$	−0.2 ± 0.1	3	this work
Brocadia spp.	NH_4SO_4 + $NaNO_2$	−0.5 ± 0.3	2	this work
Scalindua spp.	NH_4SO_4 + $NaNO_2$	1.0 ± 0.3	3	this work
denitrifying bacteria				
Pseudomonas stutzeri	KNO_3	0.9 ± 0.4	4	14
Paracoccus denitrificans	KNO_3	0.6 ± 0.2	5	14

rubber stoppers (Geomicrobial Technologies, Inc., Ochelata, OK, U.S.A.). Initially, after saturating the dried soils, an anaerobic headspace was created by sparging with He. The soils were then allowed to denitrify for 7−10 d to remove any initial oxidized N. At that point, the headspace was sparged again with He and then inoculated with glucose (0.3 mL, 1 M) and $NaNO_3$ substrate (1 mL, 0.3 M; $\delta^{15}N$ = 5.4‰). Production of N_2 was allowed to proceed for 96 h to ensure collection of sufficient N_2 gas for isotopic analysis. Gases were transferred cryogenically to a pre-evacuated silica-gel finger and flame-sealed prior to analysis at UCLA.

For the in situ study, soil gas samples from the KBS Interactions Experiment site were obtained from a monolith soil lysimeter. The lysimeter is located 5 m from the edge of Plot 13 (27 × 40 m total width), which had followed an annual corn−soybean−winter wheat rotation (conventional tillage, no fertilizer) until spring 2016, when planting was changed to Cave-in-rock switchgrass (*Panicum virgatum* L.). Constructed of stainless steel, the 2.29 × 1.22 × 2.03 m ($L \times W \times D$) monolith lysimeter was installed with a minimum of disturbance to the soil column approximately 5 cm above the soil surface in 1986 as described in Brown et al.[23] Gas sampling lines (stainless steel, 1.6 mm OD, 0.5 mm ID) were previously installed through the walls of the lysimeter and extend 30 cm outward. Each line was purged by removing 3 mL of soil gas (∼50 times the line volume) by gastight syringe and discarding the gas. Subsequently, 5 mL of gas for each sample was collected by gastight syringe and pushed through a 3 mL stainless-steel sampling bottle that had been previously purged with He gas. Gas samples were collected on 10/11/17 and 7/18/18 at depths of 24, 34, 50, 59, 77, 86, and 170 cm from the soil surface. On return to the laboratory, gases were cryogenically purified and transferred to a pre-evacuated silica-gel finger and flame-sealed.

RESULTS AND DISCUSSION

Δ_{30} Values from Biological N_2 Production Are Near Zero. Anammox enrichment cultures produced N_2 with Δ_{30} values close to, but slightly different from the stochastic distribution of isotopes (Table 1). Nitrogen gas produced by the two freshwater genera are characterized by $\Delta_{30} < 0$ (i.e., N_2 was "anticlumped"), while N_2 produced by the marine *Ca. Scalindua* enrichment had Δ_{30} = 1.0 ± 0.3‰, indistinguishable from an equilibrium distribution of ^{15}N isotopes at culturing temperatures (i.e., 1.0‰ at 35 °C). A positive correlation between Δ_{30} and $\delta^{15}N$ values was observed when all anammox culture data are considered together (R^2 = 0.86, p = 0.0009). The origins of this correlation were not investigated, but deserve further scrutiny: the apparent difference in Δ_{30} value between freshwater and marine species may point to a different biochemistry related to the gene organization and subsequent expression of hydrazine synthase enzyme.[24,25] In any case, the Δ_{30} values for N_2 produced by freshwater anammox genera are close to that expected from combinatorial isotope effects:[26] the contrast in isotopic compositions between the $NaNO_2$ ($\delta^{15}N$ = −26.2‰) and NH_4SO_4 ($\delta^{15}N$ = −0.5‰) substrates, by itself, would yield Δ_{30} = −0.2‰, close to the mean measured values of −0.2 ± 0.1‰ and −0.5 ± 0.3‰ (1σ) for *Ca. Kuenenia* and *Ca. Brocadia*, respectively. Isotopic fractionation during biological uptake[10] may cause additional variability in the $\delta^{15}N$ value of the assimilated substrates, but the Δ_{30} value of the N_2 produced is not expected to deviate more than ∼1‰ from zero because the combinatorial effect is a relatively weak function of the substrate $\delta^{15}N$ contrast.[26]

Anaerobic incubation of KBS soils yielded N_2 with Δ_{30} values indistinguishable from the stochastic distribution of isotopes (i.e., all within 0.2‰; see Table 1). Unlike in previous axenic laboratory cultures of denitrifying bacteria,[14] no statistically significant dependence on reaction extent or $\delta^{15}N$ values was observed (p = 0.2−0.4 for a slope of zero, depending on the soil; see Table S1 of the Supporting Information, SI).

Compiling these results with those from earlier experiments on bacterial denitrifiers[14] shows that biological N_2 production yields Δ_{30} values between −0.7‰ and +1.4‰, with a weak dependence, if any, on bulk $\delta^{15}N$ values (Table S1). Moreover, the lack of Δ_{30} fractionation during biological nitrogen fixation[14] suggests that it preserves Δ_{30} values in the N_2 residue. Atmospheric N_2, in contrast, is characterized by $\Delta_{30,\,atm}$ = 19.1 ± 0.1‰ (Figure 1).[14]

Using Δ_{30} Values to Detect Biological N_2 Fraction in Soil Gas. Due to the large and relatively invariant Δ_{30} contrast between atmospheric and biologically produced N_2, we suggest here that Δ_{30} values in N_2 can be used to quantify biologically produced N_2 in soils via mass balance. To illustrate this concept, we first write the two-component mixing equations for the N_2 isotopologue ratios in soil, $^{29}R_{soil}$ and $^{30}R_{soil}$, in terms of the biological N_2 fraction (f_{bio}) and the N_2 isotopologue ratios of atmospheric and biological N_2 (subscripts "atm" and "bio," respectively):

$$^{29}R_{soil} = (1 - f_{bio})\,^{29}R_{atm} + f_{bio}\,^{29}R_{bio} \quad (6)$$

$$^{30}R_{soil} = (1 - f_{bio})\,^{30}R_{atm} + f_{bio}\,^{30}R_{bio} \quad (7)$$

DOI: 10.1021/acs.est.9b00812
Environ. Sci. Technol. 2019, 53, 5168−5175

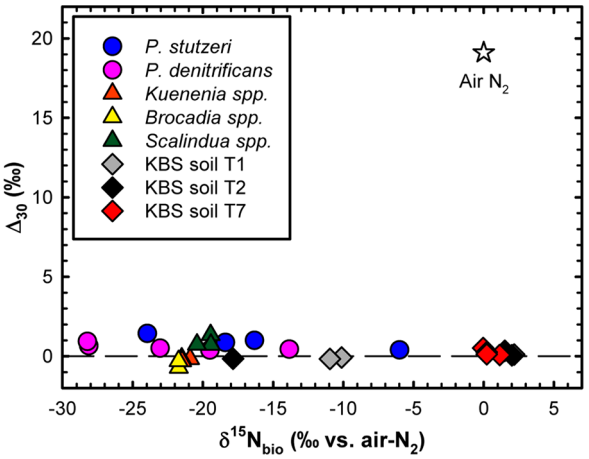

Figure 1. Clumped-isotope composition of N_2 derived from experimental cultures of denitrifying or anaerobic ammonia-oxidizing bacteria reported here and in ref 14. Substrates for experiments were as follows: USGS34 (KNO_3, $\delta^{15}N = -1.8‰$) for denitrifying bacteria, $NaNO_2$ ($\delta^{15}N = -26.2‰$) and NH_4SO_4 ($\delta^{15}N = -0.5‰$) in the anammox bioreactors, and bulk $NaNO_3$ ($\delta^{15}N = 5.4‰$) for soil incubations.

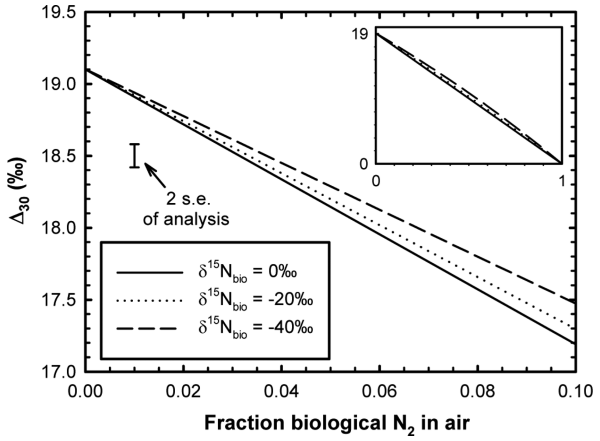

Figure 2. Effects of bulk isotopic composition of biologically produced N_2 on clumped-isotope based mass balance of biological and atmospheric N_2. Inset shows mixing nonlinearity over the entire range of mixing fractions, which is most pronounced near a biological fraction of 0.5.

While the soil-gas $^{29}R_{soil}$ and $^{30}R_{soil}$ values can be measured (as $\delta^{15}N_{soil}$ and $\Delta_{30,soil}$ values) and $^{29}R_{atm}$ and $^{30}R_{atm}$ are known, this system of equations remains under-constrained. However, the proportionality between $^{29}R_{bio}$ and $^{30}R_{bio}$ coming from a relatively invariant biological clumped-isotope signature ($\Delta_{30,bio}$) provides a way forward.

Two-component mixing is linear in Δ_{30} values if the biologically produced N_2 has the same $^{15}N/^{14}N$ ratio as that of the atmosphere, i.e., $\delta^{15}N_{bio} = \delta^{15}N_{atm}$, yielding eq 8:[14,27]

$$\Delta_{30,soil} = (1 - f_{bio})\Delta_{30,atm} + f_{bio}\Delta_{30,bio} \quad (8)$$

In that case, the soil-gas Δ_{30} value ($\Delta_{30,soil}$) would be simply related to f_{bio} and the atmospheric ($\Delta_{30,atm}$) and biological clumped-isotope signatures. Measurements of $\Delta_{30,soil}$ would allow one to solve for f_{bio}:

$$f_{bio} = \frac{\Delta_{30,atm} - \Delta_{30,soil}}{\Delta_{30,atm} - \Delta_{30,bio}} \quad (9)$$

Unknown and variable $\delta^{15}N_{bio}$ values lead to deviations from this relationship, and uncertainty in f_{bio}. However, for $\Delta_{30,soil}$ values close to $\Delta_{30,atm}$ (i.e., mixtures dominated by atmospheric N_2), eqs 8 and 9 retain much of their accuracy over a wide range of $\delta^{15}N_{bio}$ values (Figure 2). For example, when $\delta^{15}N_{bio}$ is 20‰ different from $\delta^{15}N_{atm}$, the f_{bio} value derived from eq 9 is within 6% of the true f_{bio} value (e.g., a calculated f_{bio} of 0.094 when the true f_{bio} is 0.1). The expected range of $\Delta_{30,bio}$ values coming from natural communities of ±1‰—i.e., the range observed in laboratory experiments—results in an additional ±6% relative uncertainty in f_{bio} (e.g., an error of ±0.006 for f_{bio} = 0.1). Both errors are similar to that contributed by analytical uncertainty for f_{bio} = 0.1 (resulting in a cumulative uncertainty of ±10% if added in quadrature), but they quickly decrease in importance as f_{bio} decreases: for f_{bio} = 0.01, analytical uncertainty of ±0.08‰ in Δ_{30} results in an asymmetrical uncertainty of +36% and −56% f_{bio}, i.e., $f_{bio} = 0.010^{+0.004}_{-0.006}$. Therefore, analytical uncertainty dominates Δ_{30}-based estimates of f_{bio} for f_{bio} < 0.1. Current analytical uncertainties suggest that soil gas containing ≥1% biological N_2 will be detectable in $\Delta_{30,soil}$ values.

To test this concept, we obtained two depth profiles of $\delta^{15}N$ and Δ_{30} values in N_2, along with N_2O concentrations, from a monolith lysimeter installed in the KBS Interactions site. We found that many $\Delta_{30,soil}$ values were less than or equal to $\Delta_{30,atm}$ (Figure 3 and Table S2), ranging from 18.8‰ to 19.1‰. One sample analysis (34 cm depth on 10/11/17) was rejected based on apparent contamination that resulted in an abnormally elevated Δ_{30} value (4σ above the mean atmospheric value measured during the analytical session). The largest $\Delta_{30,soil}$ depletions (−0.3 ± 0.1‰ relative to $\Delta_{30,atm}$), observed in both profiles, correspond to $1.6^{+0.4}_{-0.5}$% of soil N_2 at those depths being derived from biological processes. Soil-N_2 $\delta^{15}N$ values were equal to or slightly lower than the atmospheric value, although they differed between profiles: the profile obtained in July 2018 had $\delta^{15}N$ values close to the atmospheric value, while the profile obtained in October 2017 had subatmospheric $\delta^{15}N$ values ranging from −0.4 to −0.6‰. N_2O concentrations increased nearly monotonically with increasing depth, with values exceeding 1000 parts per billion (ppb) at 170 cm depth (Figure 4). Taken together, these data imply an active nitrogen cycle and the presence of biological N_2 in these soils.

Gas Diffusion and Denitrification Hot-Spots Can Explain Observed Soil Δ_{30} Profiles. A further understanding of the chemical and isotopic signatures measured in the soil gas can be obtained using a one-dimensional diffusion-reaction model based on Fick's second law:

$$\frac{\partial C}{\partial t} = D_z\frac{\partial^2 C}{\partial z^2} + J(z, t) \quad (10)$$

where D_z is the effective gas diffusivity and $J(z,t)$ is the production rate of a gas, which may be depth-(z) and time-(t) dependent. We treat the soil-gas system as a diffusive column ventilated to the atmosphere at the top (z = 0) and with zero permeability at the bottom (z = 180 cm). At steady state ($\partial C/\partial t = 0$) the depth profile is described by $\partial^2 C/\partial z^2 = -J/D_z$; because J and D_z are positive as defined, concentration depth profiles at steady state should monotonically decrease toward the atmospheric value. Isotopic tracers may increase or

DOI: 10.1021/acs.est.9b00812
Environ. Sci. Technol. 2019, 53, 5168−5175

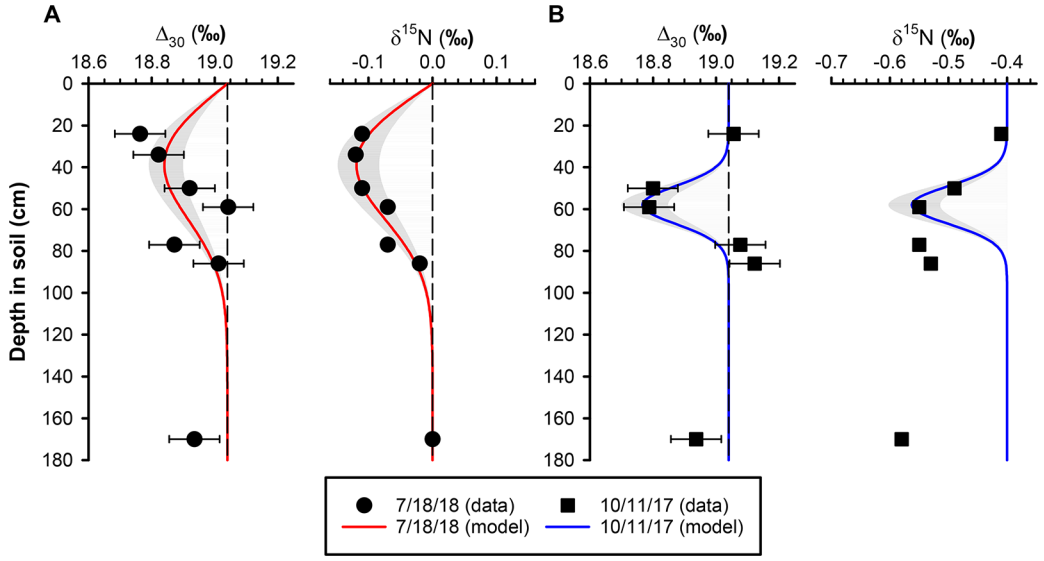

Figure 3. Depth profiles of Δ_{30} and $\delta^{15}N$ values in N_2 drawn from the same monolith lysimeter at the KBS LTER Interactions Experiment site on 7/18/18 (A) and 10/11/17 (B). Mean measured atmospheric Δ_{30} values were 19.04 ± 0.03‰ (1 s.e.m., n = 5) during the analysis period (dashed lines). Solid lines show depth profiles calculated using a 1-D diffusion-reaction model for each sampling date that are consistent with the Δ_{30} data (10/11/17 profile offset by −0.4‰). Note that these best-fit profiles for Δ_{30} may not be unique solutions due to the number of adjustable parameters in the model, e.g., the duration, width, and depth distribution of the assumed biological N_2 pulse. Shaded areas therefore represent the range of N_2 production rates that describes the analytical 1σ of Δ_{30} values (i.e., + 25% and −30% relative to the solid lines). Dashed lines denote isotopic compositions in the free atmosphere.

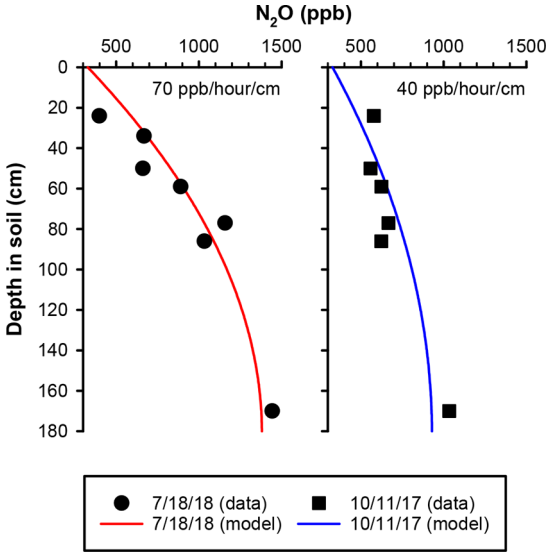

Figure 4. Depth profiles of N_2O concentrations from the same samples as shown in Figure 3, along with illustrative steady-state profiles for uniform N_2O production rates and 5% gas-filled porosities (D_z = 0.0026 cm^2 s^{-1}).[31,32]

decrease toward the top depending how they are defined, but the change with depth should be monotonic toward the atmospheric value.

The depth profiles are not in steady state with respect to N_2. At steady state, deeper soil-gas would have accumulated low-Δ_{30} biological signals over time, resulting in $\Delta_{30,soil}$ values increasing from depth to the surface. The N_2O depth profiles show accumulation at depth, but the N_2 profiles do not (Figures 3 and 4). Instead, $\Delta_{30,soil}$ values are close to atmospheric values at depth, decrease at mid-depths, and return to atmospheric values at the surface. Pulsed biological N_2 production over a limited depth range is required to reproduce these mid-depth minima in $\Delta_{30,soil}$ values. Specifically, a quiescent period with respect to N_2 production, which ventilates the soil down to 170 cm, must precede the pulse. Quantitative ventilation is not necessary, however; the quiescent period need only be long enough to dilute remnant $\Delta_{30,soil}$ signals from earlier events beyond the limits of detection (~5 days for the expected diffusivities; see below). Denitrification "hot moments" related to heterogeneities in soil moisture and organic carbon availability[28,29] have the appropriate temporal and spatial variability. The contrast between N_2 and N_2O depth profiles suggest that their production during these hot moments can be temporally decoupled. Moreover, the accumulation of N_2O at depth argues against ventilation via gas exchange at the lysimeter–soil interface as the origin of the nonsteady-state $\Delta_{30,soil}$ depth profile.

The shapes of the $\Delta_{30,soil}$ depth profiles can be reproduced by solving eq 10 using a 0.1-day N_2 production pulse of Gaussian shape (1 cm full width at half-maximum), followed

Table 2. Model Parameters Used to Derive Profiles in Figure 3[a]

sampling date	center depth (cm)	pulse peak (nmol N_2 cm^{-3} s^{-1})	sampling lag (h)	N_2 production (mmol N_2 m^{-2})
10/11/17	59	1.2	1.9	5.7
7/18/18	37	2.6	26.4	12.9

[a]Pulses are Gaussian (1 cm full width at half maximum), occurring for 0.1 days.

DOI: 10.1021/acs.est.9b00812
Environ. Sci. Technol. 2019, 53, 5168−5175

by a small time lag between the N_2 pulse and sampling (see Table 2). Here, we assume an air-filled porosity, ε, of 0.05—resulting in a calculated[30,31] soil diffusivity of D_z = 0.0039 cm^2 s^{-1} for N_2—and $\Delta_{30,bio}$ = 0. The assumed ε value is within the plausible range for these soils[32] so it is appropriate for illustrative purposes. Using these parameters, the modeled $\Delta_{30,soil}$ depth profile for July 2018 (the best-fit curve using a least-squares algorithm) reflects a depth-integrated gross production of 10.4 mmol N_2 m^{-2} remaining in the soil after a 12.9 mmol N_2 m^{-2} pulse (Figure 3A). The $\delta^{15}N$ values of N_2 in that profile can be reproduced if the biological N_2 has $\delta^{15}N$ = −11‰, on average. Note that the particular pulse shape, duration, and sampling lag used here (Table 2) is likely one of many that can explain the data and therefore not meant to be diagnostic; consequently, the profile is considered a local (rather than global) best fit. The depth-integrated gross production, however, should be robust for a given air-filled porosity. For example, the model can also yield a satisfactory fit of the data using a 10-fold longer initial N_2 pulse length of 1 day with a correspondingly weaker peak pulse peak of 0.3 nmol N_2 cm^{-3} s^{-1} (instead of 2.6 nmol N_2 cm^{-3} s^{-1}). Both scenarios yield scaled-up N_2 pulse magnitudes (3−4 kg N ha^{-1}) that are consistent with peak N_2 fluxes observed in previous in lab[33] and field[34] experiments.

The modeled Δ_{30} depth profile for October 2017 shown in Figure 3 implies a depth-integrated gross production of 5.7 mmol N_2 m^{-2} using a pulse centered at 59 cm (Figure 3B, Table 2). Unlike for the July 2018 profile, the $\delta^{15}N$ values of N_2 in that profile cannot be explained by biological N_2 production alone. Gravitational fractionation over this depth range would increase $\delta^{15}N$ values by <0.01‰, so other physical mechanisms such as diffusive fractionation and/or water vapor flux fractionation[13] may be especially important for this profile. Sampling took place the morning after a heavy overnight precipitation event (>40 mm), implicating a physical isotope effect such as a hydrologically driven diffusive influx of atmospheric N_2. These physical mechanisms will not affect $\Delta_{30,soil}$ values significantly because they fractionate proportionately over a small $\delta^{15}N$ range.[14,15] In addition, solubility fractionation does not seem to affect clumped-isotope compositions of sparingly soluble gases,[14,35] despite its effects on both elemental[36] and bulk-isotope composition.[37] Consequently, the Δ_{30} tracer shows a clearer measure of biological N_2 production than the $\delta^{15}N$ value of N_2.

If these biological N_2 pulses are isolated in time, then equivalent surface N_2 fluxes F can be derived from the reaction-diffusion models, and the results compared to previous measurements of KBS soils. For one-dimensional diffusion, the equation $F = [N_{2,bio}] \times D_z/z$ describes the instantaneous surface gas flux, where $[N_{2,bio}]$ is the concentration of biological N_2 and z is the depth from the surface. The results for z = 5 cm, the biological N_2 flux from the top 5 cm of soil, are shown in Figure 5. The flux F for the two profiles ranges from 0.1−2.9 mmol N_2 m^{-2} d^{-1} (3−81 mg N m^{-2} d^{-1}) during the first 10 days after the pulse events, with a prolonged period of low, but nonzero flux lasting several times longer (e.g., F = 0.1−0.2 mmol N_2 m^{-2} d^{-1} for the 7/18/18 profile between 10 and 20 days after the pulse). These estimates are comparable to previous amendment-stimulated N_2 production rates from these soils.[38,39] In particular, Bergsma et al. (2001) reported surface N_2 fluxes of 0.2−2.0 mmol N_2 m^{-2} d^{-1} (6−55 mg N m^{-2} d^{-1}) during a four-day experiment utilizing a surface flux chamber and an

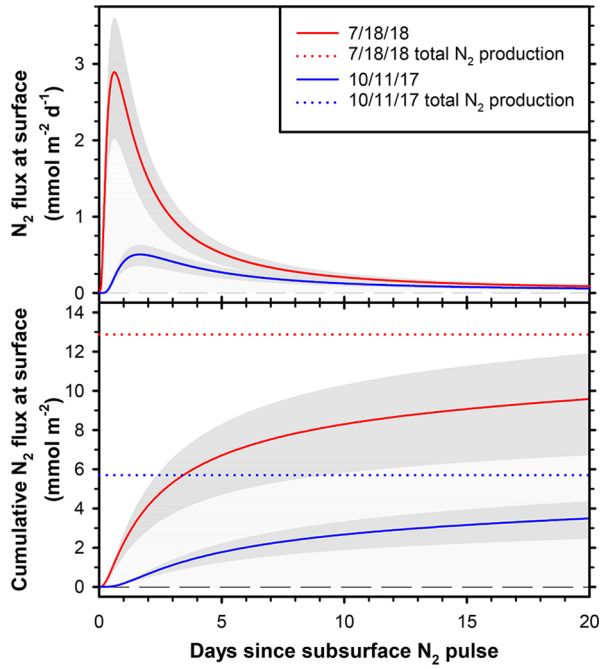

Figure 5. Calculated surface-flux time series for biological N_2 derived from the Δ_{30} depth profiles in Figure 3 (solid lines). Shaded areas represent the range of N_2 production rates that describes the analytical 1σ of Δ_{30} values (i.e., + 25% and −30% in production rate). Dotted lines represent total biological N_2 corresponding to each profile and show incomplete soil degassing after 20 days.

amendment of ^{15}N-labeled KNO_3.[38] The model-derived fluxes strongly depend on the assumed air-filled porosity ε—which was not measured directly and can vary in time and space—so this agreement may be coincidental. Nevertheless, the two methods appear to yield results on the same order of magnitude. More well constrained in situ soil-atmosphere fluxes can be obtained with concurrent measurements of soil physical properties.

The only comparable in situ method for quantifying biological N_2 production in soils is the N_2/Ar method. Yang and Silver (2012) reported a relatively high detection limit of 3.9 mmol N_2 m^{-2} d^{-1} for surface-flux measurements,[7] larger than the calculated peak surface fluxes shown in Figure 5. While the method can analytically resolve N_2 excesses of less than 0.1%,[40] physical fractionation of N_2 and Ar in soils presents substantial systematic uncertainties in these environments. We hypothesize that measurements of N_2/Ar soil profiles may yield limited improvements in uncertainty because the physical mechanisms complicating the interpretation of $\delta^{15}N$ values of N_2 (e.g., the water vapor flux fractionation)[13] fractionate N_2/Ar ratios to a greater degree, offsetting any analytical sensitivity advantages. Soil $\Delta_{30,soil}$ depth profiles, in contrast, are insensitive to physical fractionation, revealing evidence for biological N_2 production in soil profiles despite the lower analytical sensitivity of the method.

N_2 fluxes into the atmosphere can be derived from $\Delta_{30,soil}$ profiles if soil physical properties (i.e., air-filled porosity and diffusivity) are determined independently. The method could be used to compare in situ production rates to incubation- and amendment-based methods in field studies, or to obtain independent estimates using an array of spatially dispersed observations across soil types and conditions. Time series of soil-gas profiles similar to those shown here, sampled through

DOI: 10.1021/acs.est.9b00812
Environ. Sci. Technol. 2019, 53, 5168−5175

lysimeters or air-permeable tubing, would provide a long-term perspective on soil N_2 production dynamics, which is presently difficult to access without perturbing soil biogeochemistry and is useful for models.[41] Analytical throughput (2−3 samples/day) and availability of instrumentation are currently limiting factors for the Δ_{30} approach, but the relatively long ventilation time scales of certain soils may still allow weekly to-monthly sampling to capture the impacts of hot moments.

The initial results reported here suggest that $\Delta_{30,soil}$ signals are sufficiently large that the approach can be used in future assessments of site- and ecosystem-scale loss of fixed nitrogen. Furthermore, the approach can also be applied to marine environments to investigate both the magnitude and mechanisms of fixed-nitrogen loss in low-oxygen zones.[42] Finally, constraining biological N_2 production globally using $\Delta_{30,atm}$ appears possible in principle if the terms related to upper-atmospheric chemistry in the global Δ_{30} budget—both the isotopic reordering rates and Δ_{30} endmembers—can be refined.

■ ASSOCIATED CONTENT

Supporting Information

The Supporting Information is available free of charge on the ACS Publications website at DOI: 10.1021/acs.est.9b00812.

Compilation of isotopic composition data for N_2 produced during pure- and enrichment-culture experiments reported here and in ref 14; isotopic composition data for N_2 and concentrations of N_2O in soil gases (PDF)

■ AUTHOR INFORMATION

Corresponding Author

*E-mail: lyeung@rice.edu.

ORCID

Laurence Y. Yeung: 0000-0001-9901-2607

Notes

The authors declare no competing financial interest.

■ ACKNOWLEDGMENTS

This research was supported by the U.S. National Science Foundation grant EAR-1349182 to L.Y.Y. and E.D.Y., EAR-1348935 to N.E.O., the David and Lucile Packard Foundation Science & Engineering Fellowship to L.Y.Y., the Deep Carbon Observatory, The Netherlands Organization for Scientific Research Gravitation grant 024.002.002 to M.S.M.J. and Veni grant 863.14.019 to S.L. This work was funded in part by the DOE Great Lakes Bioenergy Research Center (DOE BER Office of Science DE-SC0018409). Support for this research was also provided by the NSF Long-term Ecological Research Program (DEB-1637653) at the Kellogg Biological Station and by Michigan State University AgBioResearch. We would like to thank Guylaine Nuijten for her contributions to maintaining the anammox bioreactors at Radboud University, Kevin Kahmark and Stacey Vanderwulp for their assistance with monolith lysimeter sampling, Reinhard Well for discussions, and four anonymous reviewers and the editor for comments that improved this work.

■ REFERENCES

(1) Davidson, E. A.; Seitzinger, S. The enigma of progress in denitrification research. *Ecol. Appl.* **2006**, *16*, 2057−2063.

(2) Seitzinger, S.; Harrison, J. A.; Böhlke, J. K.; Bouwman, A. F.; Lowrance, R.; Peterson, B.; Tobias, C.; Van Drecht, G. Denitrification across landscapes and waterscapes: A synthesis. *Ecol. Appl.* **2006**, *16*, 2064−2090.

(3) Yoshinari, T.; Hynes, R.; Knowles, R. Acetylene inhibition of nitrous oxide reduction and measurement of denitrification and nitrogen fixation in soil. *Soil Biol. Biochem.* **1977**, *9*, 177−183.

(4) Groffman, P. M.; Altabet, M. a.; Böhlke, J. K.; Butterbach-Bahl, K.; David, M. B.; Firestone, M. K.; Giblin, A. E.; Kana, T. M.; Nielsen, L. P.; Voytek, M. A. Methods for measuring denitrification: Diverse approaches to a difficult problem. *Ecol. Appl.* **2006**, *16*, 2091−2122.

(5) Groffman, P. M. Terrestrial denitrification: challenges and opportunities. *Ecol. Process.* **2012**, *1*, 11.

(6) Butterbach-Bahl, K.; Willibald, G.; Papen, H. Soil core method for direct simultaneous determination of N_2 and N_2O emissions from forest soils. *Plant Soil* **2002**, *240*, 105−116.

(7) Yang, W. H.; Silver, W. L. Application of the N_2/Ar technique to measuring soil-atmosphere N_2 fluxes. *Rapid Commun. Mass Spectrom.* **2012**, *26*, 449−459.

(8) Bryan, B. A.; Shearer, G.; Skeeters, J. L.; Kohl, D. H. Variable expression of the nitrogen isotope effect associated with denitrification of nitrite. *J. Biol. Chem.* **1983**, *258*, 8613−8617.

(9) Barford, C. C.; Montoya, J. P.; Altabet, M. A.; Mitchell, R. Steady-State Nitrogen Isotope Effects of N_2 and N_2O Production in *Paracoccus denitrificans*. *Appl. Environ. Microbiol.* **1999**, *65*, 989−994.

(10) Brunner, B.; Contreras, S.; Lehmann, M. F.; Matantseva, O.; Rollog, M.; Kalvelage, T.; Klockgether, G.; Lavik, G.; Jetten, M. S. M.; Kartal, B.; Kuypers, M. M. M. Nitrogen isotope effects induced by anammox bacteria. *Proc. Natl. Acad. Sci. U. S. A.* **2013**, *110*, 18994−18999.

(11) Yang, H.; Gandhi, H.; Ostrom, N. E.; Hegg, E. L. Isotopic Fractionation by a Fungal P450 Nitric Oxide Reductase during the Production of N_2O. *Environ. Sci. Technol.* **2014**, *48*, 10707−10715.

(12) Craine, J. M.; Elmore, A. J.; Wang, L.; Augusto, L.; Baisden, W. T.; Brookshire, E. N. J.; Cramer, M. D.; Hasselquist, N. J.; Hobbie, E. A.; Kahmen, A.; et al. Convergence of soil nitrogen isotopes across global climate gradients. *Sci. Rep.* **2015**, *5*, 8280.

(13) Severinghaus, J. P.; Bender, M. L.; Keeling, R. F.; Broecker, W. S. Fractionation of soil gases by diffusion of water vapor, gravitational settling, and themal diffusion. *Geochim. Cosmochim. Acta* **1996**, *60*, 1005−1018.

(14) Yeung, L. Y.; Li, S.; Kohl, I. E.; Haslun, J. A.; Ostrom, N. E.; Hu, H.; Fischer, T. P.; Schauble, E. A.; Young, E. D. Extreme enrichment in atmospheric $^{15}N^{15}N$. *Sci. Adv.* **2017**, *3*, 3.

(15) Yeung, L. Y.; Young, E. D.; Schauble, E. A. Measurements of $^{18}O^{18}O$ and $^{17}O^{18}O$ in the atmosphere and the influence of isotope-exchange reactions. *J. Geophys. Res.* **2012**, *117*, D18306.

(16) Hauck, R. D.; Melsted, S. W.; Yankwich, P. E. Use of N-isotope distribution in nitrogen gas in the study of denitrification. *Soil Sci.* **1958**, *86*, 287−291.

(17) Hauck, R. D.; Bouldin, D. R. Distribution of isotopic nitrogen in nitrogen gas during denitrification. *Nature* **1961**, *191*, 871−872.

(18) Young, E. D.; Rumble III, D.; Freedman, P.; Mills, M. A large-radius high-mass-resolution multiple-collector isotope ratio mass spectrometer for analysis of rare isotopologues of O_2, N_2, CH_4 and other gases. *Int. J. Mass Spectrom.* **2016**, *401*, 1−10.

(19) Strous, M.; Pelletier, E.; Mangenot, S.; Rattei, T.; Lehner, A.; Taylor, M. W.; Horn, M.; Daims, H.; Bartol-Mavel, D.; Wincker, P.; et al. Deciphering the evolution and metabolism of an anammox bacterium from a community genome. *Nature* **2006**, *440*, 790−794.

(20) Kartal, B.; Van Niftrik, L.; Rattray, J.; Van De Vossenberg, J. L. C. M.; Schmid, M. C.; Sinninghe Damsté, J.; Jetten, M. S. M.; Strous, M. Candidatus 'Brocadia fulgida': an autofluorescent anaerobic ammonium oxidizing bacterium. *FEMS Microbiol. Ecol.* **2008**, *63*, 46−55.

(21) Van De Vossenberg, J.; Rattray, J. E.; Geerts, W.; Kartal, B.; Van Niftrik, L.; Van Donselaar, E. G.; Sinninghe Damsté, J. S.; Strous, M.; Jetten, M. S. M. Enrichment and characterization of marine

anammox bacteria associated with global nitrogen gas production. *Environ. Microbiol.* **2008**, *10*, 3120−3129.
(22) Crum, J. R.; Collins, H. P. *Kellogg Biological Station Long-Term Ecological Research.*; Michigan State University: Hickory Corners, MI, 1995.
(23) Brown, K. W.; Gerard, C. J.; Hipp, B. W.; Ritchie, J. T. Procedure for placing large undisturbed monoliths in lysimeters. *Soil Sci. Soc. Am. J.* **1974**, *38*, 981−983.
(24) Kartal, B.; Maalcke, W. J.; de Almeida, N. M.; Cirpus, I.; Gloerich, J.; Geerts, W.; Op den Camp, H. J. M.; Harhangi, H. R.; Janssen-Megens, E. M.; Francoijs, K.-J.; Stunnenberg, H. G.; Keltjens, J. T.; Jetten, M. S. M.; Strous, M. Molecular mechanism of anaerobic ammonium oxidation. *Nature* **2011**, *479*, 127−130.
(25) van de Vossenberg, J.; Woebken, D.; Maalcke, W. J.; Wessels, H. J. C. T.; Dutilh, B. E.; Kartal, B.; Janssen-Megens, E. M.; Roeselers, G.; Yan, J.; Speth, D.; et al. The metagenome of the marine anammox bacterium 'Candidatus Scalindua profunda' illustrates the versatility of this globally important nitrogen cycle bacterium. *Environ. Microbiol.* **2013**, *15*, 1275−1289.
(26) Yeung, L. Y. Combinatorial effects on clumped isotopes and their significance in biogeochemistry. *Geochim. Cosmochim. Acta* **2016**, *172*, 22−38.
(27) Eiler, J. M. Clumped-isotope" geochemistry – The study of naturally-occurring, multiply-substituted isotopologues. *Earth Planet. Sci. Lett.* **2007**, *262*, 309−327.
(28) Parkin, T. B. Soil Microsites as a Source of Denitrification Variability. *Soil Sci. Soc. Am. J.* **1987**, *51*, 1194−1199.
(29) Kravchenko, A. N.; Toosi, E. R.; Guber, A. K.; Ostrom, N. E.; Yu, J.; Azeem, K.; Rivers, M. L.; Robertson, G. P. Hotspots of soil N_2O emission enhanced through water absorption by plant residue. *Nat. Geosci.* **2017**, *10*, 496−500.
(30) Winn, E. B. The temperature dependence of the self-diffusion coefficients of argon, neon, nitrogen, oxygen, carbon dioxide, and methane. *Phys. Rev.* **1950**, *80*, 1024−1027.
(31) Millington, R. J. Gas diffusion in porous media. *Science* **1959**, *130*, 100−102.
(32) Shcherbak, I.; Robertson, G. P. Determining the Diffusivity of Nitrous Oxide in Soil using In Situ Tracers. *Soil Sci. Soc. Am. J.* **2014**, *78*, 79−88.
(33) Meijide, A.; Cardenas, L. M.; Bol, R.; Bergstermann, A.; Goulding, K.; Well, R.; Vallejo, A.; Scholefield, D. Dual isotope and isotopomer measurements for the understanding of N_2O production and consumption during denitrification in an arable soil. *Eur. J. Soil Sci.* **2010**, *61*, 364−374.
(34) Buchen, C.; Lewicka-Szczebak, D.; Fuß, R.; Helfrich, M.; Flessa, H.; Well, R. Fluxes of N_2 and N_2O and contributing processes in summer after grassland renewal and grassland conversion to maize cropping on a Plaggic Anthrosol and a Histic Gleysol. *Soil Biol. Biochem.* **2016**, *101*, 6−19.
(35) Li, B.; Yeung, L. Y.; Hu, H.; Ash, J. L. Kinetic and equilibrium fractionation of O_2 isotopologues during air-water gas transfer and implications for tracing biological oxygen cycling in the ocean. *Mar. Chem.* **2019**, *210*, 61−71.
(36) Hamme, R. C.; Emerson, S. R. The solubility of neon, nitrogen, and argon in distilled water and seawater. *Deep Sea Res., Part I* **2004**, *51*, 1517−1528.
(37) Klots, C. E.; Benson, B. B. Isotope Effect in the Solution of Oxygen and Nitrogen in Distilled Water. *J. Chem. Phys.* **1963**, *38*, 890−892.
(38) Bergsma, T. T.; Ostrom, N. E.; Emmons, M.; Robertson, G. P. Measuring Simultaneous Fluxes from Soil of N_2O and N_2 in the Field using ^{15}N-Gas "Nonequilbrium" Technique. *Environ. Sci. Technol.* **2001**, *35*, 4307−4312.
(39) Bergsma, T. T.; Robertson, G. P.; Ostrom, N. E. Influence of Soil Moisture and Land Use History on Denitrification End-Products. *J. Environ. Qual.* **2002**, *31*, 711−717.
(40) Hamme, R. C.; Emerson, S. Deep-sea nutrient loss inferred from the marine dissolved N_2/Ar ratio. *Geophys. Res. Lett.* **2013**, *40*, 1149−1153.
(41) Denk, T. R. A.; Kraus, D.; Kiese, R.; Butterbach-Bahl, K.; Wolf, B. Constraining N cycling in the ecosystem model LandscapeDNDC with the stable isotope model SIMONE. *Ecology* **2019**, *100*, No. e02675.
(42) Fuchsman, C. A.; Devol, A. H.; Casciotti, K. L.; Buchwald, C.; Chang, B. X.; Horak, R. E. A. An N isotopic mass balance of the Eastern Tropical North Pacific oxygen deficient zone. *Deep Sea Res., Part II* **2018**, *156*, 137−147.

DOI: 10.1021/acs.est.9b00812
Environ. Sci. Technol. 2019, 53, 5168−5175